Giant Nonadiabatic Effects in Layer Metals: Raman Spectra of Intercalated Graphite Explained

A. Marco Saitta, Michele Lazzeri, Matteo Calandra, and Francesco Mauri

IMPMC, Universités Paris 6 et 7, CNRS, IPGP, 140 rue de Lourmel, 75015 Paris, France

(Received 29 February 2008; published 2 June 2008)

The occurrence of nonadiabatic effects in the vibrational properties of metals has been predicted since the 1960s, but hardly confirmed experimentally. We report the first fully *ab initio* calculations of nonadiabatic frequencies of a number of conventional (hcp Ti and Mg) and layered metals (MgB_2, CaC_6, and other intercalated graphites). Nonadiabatic effects can be spectacularly large (up to 30% of the phonon frequencies) in both cases, but they can only be experimentally observed in the Raman spectra of layered compounds. In layered metals nonadiabatic effects are crucial to explaining the observed Raman shifts and linewidths. Moreover, we show that those quantities can be used to extract the electron momentum-relaxation time.

DOI: 10.1103/PhysRevLett.100.226401 PACS numbers: 71.15.Mb, 63.20.dk, 63.20.kd, 74.70.Ad

The adiabatic Born-Oppenheimer approximation is the state of the art in first-principles calculations of vibrational properties in solids. In metals, even if in principle unjustified, this approximation generally leads to phonon dispersions in very good agreement with experimental data [1]. Indeed violations of the adiabatic Born-Oppenheimer approximation are hardly visible in solids. Engelsberg and Schrieffer suggested [2] that nonadiabatic (NA) effects could lead to a significant renormalization of zone-center optical phonon frequencies. An intense effort has been devoted to detect measurable NA effects in metals, mainly by Raman spectroscopy [3–5]. In fact, Raman spectroscopy allows the determination of phonon frequencies in metals although the corresponding cross sections are weak because of the small penetration length of light. The detected NA phonon frequencies are typically some percent larger than the adiabatic phonon frequencies.

Recently it has been shown that NA effects are crucial to interpret the dependence of Raman spectra on doping [6,7] in graphene and on doping [8,9] and on diameter and temperature [10] in nanotubes. However, despite being a central issue for the physics of graphene-based systems, the NA phonon frequency shift $\Delta\omega$ (the difference between adiabatic and NA phonon frequencies), although measurable, is less than 1% of the adiabatic phonon frequency. Moreover, these systems have lower dimensionality and a peculiar electronic structure; it is then unclear whether sizable NA effects can actually be observed in truly three-dimensional bulk metals.

Layer metallic materials, such as graphite intercalated compounds (GICs), are three-dimensional (3D) metals possessing a considerable anisotropy along one direction. Variation of the interlayer distance by intercalation or applied pressure allows one to bridge the gap between two-dimensional monolayer systems (such as graphene) and truly three-dimensional systems [11]. Thus these metals are ideal to judge the role of reduced dimensionality in determining nonadiabatic effects. CaC_6 is also an 11.5 K superconductor [12] with an intermediate electron-phonon coupling $\lambda \approx 0.83$ [13]. Most interestingly, the recent measurement of CaC_6 Raman spectrum [14] shows that the phonon frequencies related to in-plane C vibrations are almost 80 cm^{-1} larger than those obtained from density-functional theory (DFT) adiabatic calculations. This result is puzzling since in graphite the adiabatic result for the E_{2g} phonon frequency is 1577 cm^{-1}, in excellent agreement with the experimental value of 1582 cm^{-1}.

In this Letter we develop a first-principles theoretical framework to calculate the magnitude of NA effects on zone-center optical phonons in metals. We identify the general conditions for having sizable adiabatic effects in 3D bulk metals and analyze the experimental constraints that can hinder the observation of NA effects. We demonstrate that the occurrence of NA effects is not limited to reduced dimensionality, but it is a general property of metals. We apply our approach to GICs, MgB_2 and bulk metals, finding giant NA effects. To our knowledge, this is the first systematic implementation and study of nonadiabatic effects within first-principles.

Nonadiabatic effects due to the treatment of the electron-phonon coupling in the Migdal approximation (neglecting of vertex corrections in the adiabatic limit) are usually of the order $\sqrt{m/M}$, where m and M are the electronic and ionic mass, respectively, and thus generally very small. Engelsberg and Schrieffer showed that NA renormalization of adiabatic phonon frequencies, a larger effect, unrelated to the neglecting of vertex corrections, and not of the order of $\sqrt{m/M}$, can be observed if the following two conditions are satisfied [2,3]:

$$|\mathbf{q}\cdot\mathbf{v}_F| \ll \omega \tag{1}$$

$$\hbar\omega \gg \sigma, \tag{2}$$

where $\mathbf{v}_F$ is the Fermi velocity, $\mathbf{q}$ is the phonon wave vector, ω is the phonon frequency, $\sigma = \hbar/\tau$, and τ is the electron momentum-relaxation time (Drude) of the electrons near the Fermi surface due to all possible momentum-exchange scattering mechanisms.

The first condition is verified for optical phonons of small wave vector whose phase velocity is larger than the electronic Fermi velocity. Even if in principle Eq. (1) can be fulfilled in any system, provided $\mathbf{q}$ is small enough, in practice the penetration length of the laser light limits the smallest exchanged $\mathbf{q}$ in Raman experiments. The fact that Eq. (1) is experimentally difficult to satisfy in 3D metals explains why the observation of NA effects in these systems has been somehow disappointing.

The second condition states that the electron momentum-relaxation time must be much larger than the phonon period. This implies that the electron band-population dynamic is too slow to follow the atomic motion and thus the dynamic is nonadiabatic [7]. Equation (2) is usually verified in pure and well crystallized samples at low temperature. Thus Eq. (1) is the main limitation to the observation of NA effects.

This limitation can be circumvented considering a system having small $\mathbf{v}_F$ along certain directions. For example layered metals are usually characterized by a small $\mathbf{v}_F$ component perpendicular to the layers. Since the samples are usually cleaved parallel to the layers and Raman experiments are performed perpendicularly to the freshly cleaved surface, the scalar product $\mathbf{q}\cdot\mathbf{v}_F$ is small. It is instead also evident that condition (1) is easily verified in 2D or 1D systems, since Raman experiments are performed with an incident light of wave vector $\mathbf{q}$ perpendicular to the sample spatial dimension(s) and, thus, to $\mathbf{v}_F$. In fact, NA effects have been consistently observed in doped graphene and nanotubes in the past few years [6–9].

NA effects can be taken into account by applying time-dependent perturbation theory to DFT. Neglecting the electron momentum-scattering rate ($\sigma = 0$), the dynamical matrix ($\mathcal{D}$) for a phonon at $\mathbf{q} = \mathbf{0}$ ($\mathbf{\Gamma}$) and the first-order variation of the electronic charge density (Δn) are [15]

$$\mathcal{D}_{\mathbf{\Gamma}}(\omega) = \frac{2}{N_{\mathbf{k}}}\sum_{\mathbf{k}n,m\neq n}\frac{|D_{\mathbf{k}m,\mathbf{k}n}|^2[f_{\mathbf{k}m}-f_{\mathbf{k}n}]}{\epsilon_{\mathbf{k}m}-\epsilon_{\mathbf{k}n}+\hbar\omega} + \int n(\mathbf{r})\Delta^2 V^b(\mathbf{r})d\mathbf{r} - \int \Delta n_{\mathbf{\Gamma}}(\mathbf{r},\omega)K(\mathbf{r},\mathbf{r}')\Delta n_{\mathbf{\Gamma}}(\mathbf{r},\omega)d\mathbf{r}d\mathbf{r}' \quad (3)$$

$$\Delta n_{\mathbf{\Gamma}}(\mathbf{r},\omega) = \frac{2}{N_{\mathbf{k}}}\sum_{\mathbf{k}n,m\neq n}\frac{\langle\mathbf{k}n|\mathbf{r}\rangle\langle\mathbf{r}|\mathbf{k}m\rangle D_{\mathbf{k}m,\mathbf{k}n}[f_{\mathbf{k}m}-f_{\mathbf{k}n}]}{\epsilon_{\mathbf{k}m}-\epsilon_{\mathbf{k}n}+\hbar\omega}, \quad (4)$$

where $n(\mathbf{r})$ is the charge density, the summation is performed on $N_{\mathbf{k}}$ k points, $D_{\mathbf{k}m,\mathbf{k}n} = \langle\mathbf{k}m|\Delta V^{sc}|\mathbf{k}n\rangle$ is the deformation potential proportional to the electron-phonon matrix element, ΔV^{sc} and $\Delta^2 V^b$ are, respectively, the first derivative of the Kohn-Sham potential and the second derivative of the bare (purely ionic) potential with respect to the phonon displacement. The kernel $K(\mathbf{r},\mathbf{r}')$ is the second functional derivative of the Hartree exchange and correlation potential with respect to the densities at $\mathbf{r}$ and $\mathbf{r}'$. Finally, $f_{\mathbf{k}n}$ is the Fermi function for a Bloch state $|\mathbf{k}n\rangle$ having band energy $\epsilon_{\mathbf{k}n}$. The NA frequencies have to be computed self-consistently from $\omega^{\mathrm{NA}} = \sqrt{\mathcal{D}_{\mathbf{\Gamma}}(\omega^{\mathrm{NA}})/M}$. Since in Eqs. (3) and (4) only interband transitions contribute, if $\hbar\omega^{\mathrm{NA}} \ll |\epsilon_{\mathbf{k}e} - \epsilon_{\mathbf{k}o}|$, i.e., if the phonon energy is much smaller than the direct gap between empty ($\epsilon_{\mathbf{k}e}$) and occupied ($\epsilon_{\mathbf{k}o}$) states, $\mathcal{D}_{\mathbf{\Gamma}}(\omega^{\mathrm{NA}}) \simeq \mathcal{D}_{\mathbf{\Gamma}}(0)$. We verified numerically that in all systems considered in the present study this approximation applies and that the results obtained with $\mathcal{D}_{\mathbf{\Gamma}}(\omega^{\mathrm{NA}})$ and $\mathcal{D}_{\mathbf{\Gamma}}(0)$ are indistinguishable.

The adiabatic frequency ω^A is as usual calculated within static perturbation theory, as in Ref. [1]. Note that $\omega^A \neq \sqrt{\mathcal{D}_{\mathbf{\Gamma}}(0)/M}$ since in the adiabatic case the intraband ($m = n$) term is present [6] and $\Delta\omega = \omega^{\mathrm{NA}} - \omega^A$ is

$$\hbar\,\Delta\omega \simeq \frac{1}{N_{\mathbf{k}}}\sum_{\mathbf{k}n}\frac{\hbar|D_{\mathbf{k}n,\mathbf{k}n}|^2}{M\omega^A}\delta(\epsilon_F - \epsilon_{\mathbf{k}n}) = n(\epsilon_F)\overline{g^2(\epsilon_F)}, \quad (5)$$

where $n(\epsilon_F)$ is the density of states at the Fermi level, $g^2(\epsilon_f) = \hbar|D_{\mathbf{k}n,\mathbf{k}n}|^2/2M\omega^A$ is the square electron-phonon matrix element due to intraband transitions, and $\overline{g^2(\epsilon_F)}$ is the average of $g^2(\epsilon_f)$ over the Fermi surface.

We apply our first-principles approach to obtain E_{2g} [16] nonadiabatic phonon frequencies at $\mathbf{\Gamma}$ for a number of GICs, for MgB_2 and for bulk hcp Ti (see [17] for computational details). The results are illustrated in Fig. 1 for GICs and are collected in Table I for all the systems. In general, huge $\Delta\omega$ values ($>60\ \mathrm{cm}^{-1}$) are found in all layered compounds. The most spectacular nonadiabatic effects are found in KC_8 ($\Delta\omega = 310\ \mathrm{cm}^{-1}$, 20% of ω^A) and in MgB_2 ($\Delta\omega = 230\ \mathrm{cm}^{-1}$, 30% of ω^A). Even in bulk Ti we find a significant shift, $\Delta\omega = 12\ \mathrm{cm}^{-1}$ (more than 8% of ω^A). Interestingly, despite the structural similarity, in bulk Mg no NA effect exists. From Fig. 1 the experimental Raman data [19–23] in all GICs are in much closer agreement with ω^{NA} than with ω^A, whereas in MgB_2 Raman data lie between the two theoretical frequencies. In Ti,

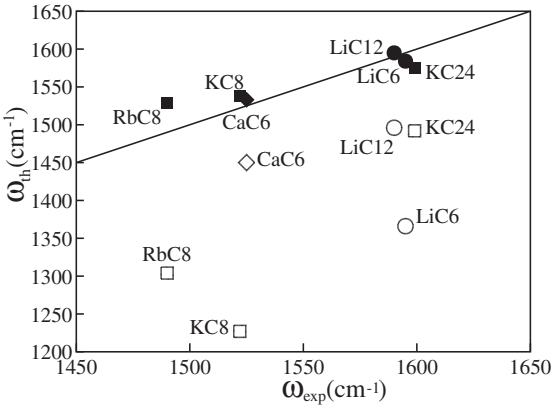

FIG. 1. Calculated adiabatic (open symbols) and nonadiabatic (solid symbols) E_{2g} [16] frequencies of several GICs, compared to measurements. The line is the 1:1 ratio.

TABLE I. Calculated adiabatic and nonadiabatic E_{2g} [16] phonon frequencies, experimental frequencies, calculated $\Delta\omega = \omega^{NA} - \omega^{A}$, calculated σ, calculated electron-phonon coupling (EPC) linewidth, experimental linewidth of several GICs and of MgB_2 (all in cm^{-1}). Measurements are from Refs. [14,19–25]. For Mg and Ti σ cannot be determined from our theory. Since our best NA frequency of graphite is 1578 cm^{-1}, we have upshifted by 4 cm^{-1} all the adiabatic/NA frequencies of GICs.

	ω^A	ω^{NA}	ω_{exp}	$\Delta\omega$	σ	γ_σ^{EPC}	Γ_{exp}
LiC_6	1362	1580	1595	218	0	0	70
LiC_{12}	1492	1591	1590	99	151	20	66
KC_8	1223	1534	1522	311	245	120	157
KC_{24}	1488	1571	1599	83	0	0	26
RbC_8 4 K	1300	1525	1490	225	558	163	100
RbC_8 77 K	1300	1525	1480	225	650	180	120
CaC_6 5 K	1446	1529	1525	83	325	36	71
CaC_6 300 K	1446	1529	1511	83	761	68	111
SrC_6	1459	1530	⋯	71	⋯	⋯	⋯
BaC_6	1462	1521	⋯	59	⋯	⋯	⋯
MgB_2 21 K	538	761	600	224	867	199	197
Mg	122	123	122.5	1	*	*	*
Ti	139	151	141	12	*	*	*

contrary to the layered metals, the observed Raman frequencies [26] are much closer to the adiabatic value.

To refine our model, we now compute phonon frequencies in the presence of a finite electron momentum-relaxation rate σ, $\omega^\sigma = \omega^A + \Delta\omega^\sigma$. $\Delta\omega^\sigma$ can be obtained using electron and hole Green functions dressed by the interaction (electron-electron, electron-phonon, and electron-defect) in the calculation of the phonon self-energy and of the dynamical matrix [3,27]. Assuming (i) σ independent of energy and (ii) $n(\epsilon)$ and $g(\epsilon_f)$ constants for bands within $\epsilon_F \pm \sigma$, Refs. [3,27] obtained

$$\hbar\,\Delta\omega^\sigma \simeq \hbar\Delta\omega\,\frac{(\hbar\omega^A)^2}{(\hbar\omega^A)^2 + \sigma^2}. \tag{6}$$

Note that when $\hbar\omega^A \gg \sigma$, $\Delta\omega^\sigma \simeq \Delta\omega$ and the experimentally observed phonon frequency is ω^{NA}; i.e., the system is in the purely NA regime. On the contrary, for $\hbar\omega^A \ll \sigma$, $\Delta\omega^\sigma = 0$ and the measured phonon frequency is ω^A; i.e., the system is completely adiabatic.

The linewidth of an optical phonon mode at $\mathbf{\Gamma}$ is also affected by the presence of a finite momentum-relaxation rate. The decay of a phonon into noninteracting (undressed) electron-hole pairs ($\sigma = 0$) is forbidden for a zone-center optical mode if the direct gap is larger than the phonon energy ($\hbar\omega \ll |\epsilon_{\mathbf{k}e} - \epsilon_{\mathbf{k}o}|$). This condition has been verified in all layered systems considered here, thus a zero linewidth should be measured [28,29]. However in all stage-1 GICs and in MgB_2, very large linewidths, hardly explainable in term of anharmonicities, are measured. Analogously to the calculation of ω^σ, a finite momentum-scattering rate σ can be considered in the evaluation of the imaginary part of the phonon self-energy [3,27,30]. This leads to the following expression for the phonon full linewidth at half maximum due to the phonon decay in dressed electron-hole pairs (γ_σ^{EPC}):

$$\frac{\gamma_\sigma^{EPC}}{2} \simeq \hbar\Delta\omega\,\frac{\sigma\hbar\omega^A}{(\hbar\omega^A)^2 + \sigma^2}. \tag{7}$$

Equation (6) can be used to extract σ. Setting $\Delta\omega^\sigma = \omega_{exp} - \omega^A$, we obtain σ from the inversion of Eq. (6). Then σ is inserted in Eq. (7) to determine γ_σ^{EPC} and the results are reported in Table I. The comparison between γ_σ^{EPC} and the experimental Raman linewidths Γ_{exp} is in Fig. 2. The agreement is overall very good, except for LiC_6 and RbC_8. Note that the experimental linewidth includes all sorts of broadening (including inhomogeneous effects), while γ_σ^{EPC} includes only the phonon decay into dressed electron-hole pairs. Thus when $\Gamma_{exp} \approx \gamma_\sigma^{EPC}$ the dominant broadening is the latter one. This is the case in MgB_2 [30,31], and in most GICs. Moreover, by comparing with the universal curves of Eqs. (6) and (7) (Fig. 3), we deduce that our estimate of the relaxation time is a good indicator of the nonadiabaticity degree.

As an example, our results quantitatively indicate that MgB_2, although being characterized by a huge $\Delta\omega$, has a smaller $\Delta\omega^\sigma$ and a relatively short momentum-relaxation time. It is thus a mostly adiabatic system, even though $\Delta\omega^\sigma$ is still very large. On the contrary, all GICs have relatively small σ's, falling in the left part of the universal curves of Fig. 3, and are thus mostly nonadiabatic. The result on hcp Ti actually indicates that all metals might have NA frequencies at $\mathbf{\Gamma}$ significantly different from the adiabatic ones, but that they cannot be observed by Raman spectroscopy because the condition (1) is not verified in experiments. In other words, nonadiabaticity is not a

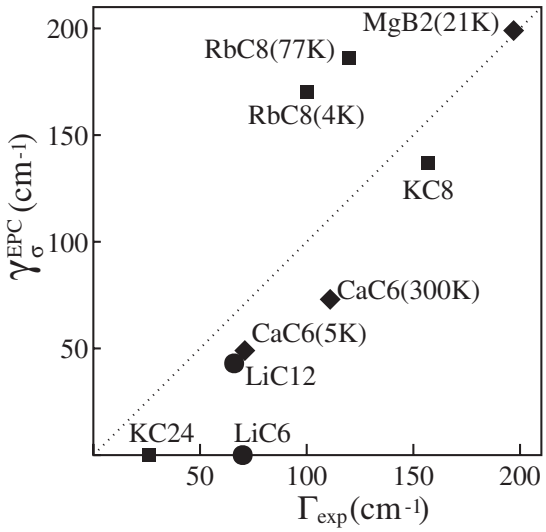

FIG. 2. Calculated EPC linewidths [Eq. (7)] versus total measured ones.

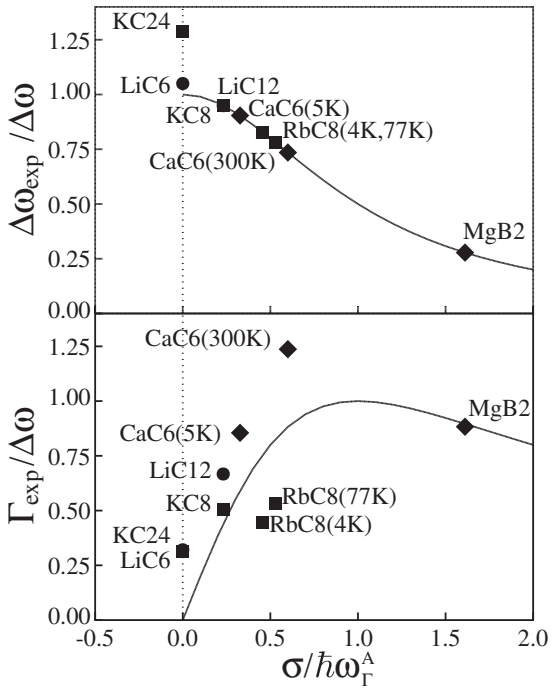

FIG. 3. Top: $\hbar\Delta\omega_\sigma/\hbar\Delta\omega$ [Eq. (6), solid line], compared to measured frequencies (symbols). Bottom: $\gamma_\sigma^{EPC}/\hbar\Delta\omega$ [Eq. (7), solid line], and measured linewidths (FWHM).

unique property of low-dimensional or layered systems, and can occur even in conventional metals.

In conclusion, we provide a quantitative first-principles theoretical framework to explain the difference between the reported experimental E_{2g} [16] mode frequencies and the (ordinary) adiabatic calculated ones in several layered metals. We have shown that giant nonadiabatic effects occur in these systems. NA effects are in principle very relevant even in bulk metals, but difficult to measure. Finally, the electron momentum-relaxation time can be extracted from Raman line positions and widths and is a good indicator of the degree of nonadiabaticity.

Calculations were done at IDRIS (CP9-71387).

[1] S. Baroni, S. de Gironcoli, A. D. Corso, and P. Giannozzi, Rev. Mod. Phys. **73**, 515 (2001).
[2] S. Engelsberg and J. R. Schieffer, Phys. Rev. **131**, 993 (1963).
[3] E. G. Maksimov and S. V. Shulga, Solid State Commun. **97**, 553 (1996).
[4] Y. S. Ponosov, G. A. Bolotin, C. Thomsen, and M. Cardona, Phys. Status Solidi B **208**, 257 (1998).
[5] G. A. Bolotin *et al.*, Phys. Solid State **43**, 1801 (2001).
[6] M. Lazzeri and F. Mauri, Phys. Rev. Lett. **97**, 266407 (2006).
[7] S. Pisana *et al.*, Nat. Mater. **6**, 198 (2007).
[8] N. Caudal, A. M. Saitta, M. Lazzeri, and F. Mauri, Phys. Rev. B **75**, 115423 (2007).
[9] A. Das *et al.*, Phys. Rev. Lett. **99**, 136803 (2007).
[10] S. Piscanec *et al.*, Phys. Rev. B **75**, 035427 (2007).
[11] M. Calandra and F. Mauri, Phys. Rev. B **74**, 094507 (2006).
[12] T. E. Weller *et al.*, Nature Phys. **1**, 39 (2005).
[13] M. Calandra and F. Mauri, Phys. Rev. Lett. **95**, 237002 (2005).
[14] J. Hlinka *et al.*, Phys. Rev. B **76**, 144512 (2007).
[15] For simplicity, have identical masses M.
[16] For GICs we consider the Raman-active in-plane stretching mode having a displacement pattern corresponding to the high-energy graphite E_{2g} mode.
[17] We focus on several stable lithium, potassium, rubidium, calcium, barium, and strontium GICs, at stages 1 or 2 of intercalation, as well as on MgB_2. We study stage-1 GICs LiC_6, KC_8, RbC_8, CaC_6, BaC_6, and SrC_6, and stage-2 LiC_{12} and KC_{24}. Calculations are based on DFT, within the plane-wave/pseudopotential scheme implemented in the PWSCF code [18]. We use a Perdew-Burke-Erzherhof gradient corrected functional and ultrasoft pseudopotentials. The plane-wave energy cutoffs are between 35 and 60 Ry, according to the system. We use the experimental structural parameters for GICs containing Li [19], K and Rb [20], Ca, Ba, and Sr [11], and for MgB_2 [11]. For KC_8 and RbC_8 phonon calculations were performed by adopting $A\alpha A\alpha$ stacking since the energy differences with respect to the $A\alpha A\beta A\gamma A\delta$ stacking are negligible. Analogously, in the case of stage-2 KC_{24} a slightly different unit cell was adopted for the phonon calculations rather than the K_2C_{48} unit cell suggested in [20]. Electronic integrations were done on regular grids from $(8\times8\times4)$ to $(64\times64\times24)$ k points. We use a Methfessel-Paxton electronic smearing of 0.01 Ry. The numerical results reported are obtained with $\mathcal{D}_\Gamma(0)$, since the k-point-sampling convergence is faster than for $\mathcal{D}_\Gamma(\omega^{NA})$.
[18] S. Baroni *et al.*, www.quantum-espresso.org.
[19] D. Guérard and C. Hérold, Carbon **13**, 337 (1975).
[20] M. S. Dresselhaus and G. Dresselhaus, Adv. Phys. **51**, 1 (2002).
[21] P. C. Eklund, G. Dresselhaus, M. S. Dresselhaus, and J. E. Fischer, Phys. Rev. B **16**, 3330 (1977).
[22] P. C. Eklund, G. Dresselhaus, M. S. Dresselhaus, and J. E. Fischer, Phys. Rev. B **21**, 4705 (1980).
[23] G. L. Doll, P. C. Eklund, and J. E. Fischer, Phys. Rev. B **36**, 4940 (1987).
[24] J. W. Quilty, S. Lee, A. Yamamoto, and S. Tajima, Phys. Rev. Lett. **88**, 087001 (2002).
[25] G. L. Doll, M. H. Yang, and P. C. Eklund, Phys. Rev. B **35**, 9790 (1987).
[26] C. Stassis, D. Arch, B. N. Harmon, and N. Wakabayashi, Phys. Rev. B **19**, 181 (1979).
[27] F. Marsiglio, R. Akis, and J. P. Carbotte, Phys. Rev. B **45**, 9865 (1992).
[28] O. Jepsen *et al.*, Phys. Rev. B **51**, 3961 (1995).
[29] M. Calandra and F. Mauri, Phys. Rev. B **71**, 064501 (2005).
[30] E. Cappelluti, Phys. Rev. B **73**, 140505 (2006).
[31] M. Calandra, M. Lazzeri, and F. Mauri, Physica (Amsterdam) **456C**, 38 (2007).